



**HAL**  
open science

# Control laws for pneumatic cylinder in order to emulate the Loss Of Resistance principle

Thibault Senac, Arnaud Lelevé, Richard Moreau

## ► To cite this version:

Thibault Senac, Arnaud Lelevé, Richard Moreau. Control laws for pneumatic cylinder in order to emulate the Loss Of Resistance principle. 20th IFAC World Congress, IFAC, Jul 2017, Toulouse, France. hal-01506823

**HAL Id: hal-01506823**

**<https://hal.science/hal-01506823>**

Submitted on 7 Jan 2019

**HAL** is a multi-disciplinary open access archive for the deposit and dissemination of scientific research documents, whether they are published or not. The documents may come from teaching and research institutions in France or abroad, or from public or private research centers.

L'archive ouverte pluridisciplinaire **HAL**, est destinée au dépôt et à la diffusion de documents scientifiques de niveau recherche, publiés ou non, émanant des établissements d'enseignement et de recherche français ou étrangers, des laboratoires publics ou privés.

# Control laws for pneumatic cylinder in order to emulate the Loss Of Resistance principle

Thibault SÉNAC\* Arnaud LELEVÉ\* Richard MOREAU\*

\* Laboratoire Ampère, UMR CNRS 5005 INSA-Lyon, Université de Lyon

---

**Abstract:** Medicine requires advanced teaching methods in order to reach an efficient student training without having to train them directly on patients. In France, the Haute Autorité de la Santé (H.A.S.) has stated to "never [do] the first time with a patient" as a requirement for the training of new doctors. The goal of this work is to offer a novel robotic solution to teach students how to perform an epidural anaesthesia. This medical operation can be divided into two different gestures: first the insertion of a needle between two vertebrae and second the application of pressure on the plunger throughout the insertion of the needle. This work aims at simulating this second part as the first part has already been simulated in previous studies. We introduce a way to emulate the principle of loss of resistance felt by the anaesthetist when the needle reaches the appropriate depth. In order to reproduce the real syringe and its behaviour we propose to use a pneumatic cylinder because of the inherent quality of such an actuator. Indeed, pneumatic actuators have an inherent compliance that is interesting when creating an haptic interface. For instance, it has been used before to create a childbirth simulator.

*Keywords:* Simulators, Nonlinear control system

---

## 1. INTRODUCTION

Epidural anaesthesia, as many other medical specialties, requires a lot of training to be mastered enough to practice it on a real patient. A study by Vaughan et al. (2013) on epidural simulation reported that it required at least 80 anaesthesia to reach a 90% success rate. Thus, such a gesture requires advanced learning process. This is why this article introduces a way of simulating a part of the gesture, in order to train new anesthetist in the future.

During an epidural anaesthesia, the anaesthetist applies a constant pressure on the plunger of the syringe to indirectly locate the epidural space to inject the anaesthetic. During the insertion of the needle between two vertebrae of a patient the anaesthetist may feel an important resistance force which greatly decreases as soon as the needle reaches the epidural space. This is called the principle of *Loss Of Resistance* (LOR). This work introduces various control laws that aim at emulating this principle.

Some epidural simulators developed prior to this work also included a simulation of the LOR principle (Dang et al. (2001) and Magill et al. (2004)) but these simulations did not offer a precise emulation of the LOR principle, only using a valve with a binary type control. The valve is half-closed to create a high resistance and opened to create the loss of resistance. To emulate the phenomenon, we propose to use a pneumatic cylinder controlled by a servo-valve, using two different control patterns. This will enable a more precise control over the haptic feedback the simulator provides. This paper depicts the experimental results obtained with both control laws and it compares both solutions. In order to keep the paper short, stability

demonstrations are not detailed (they can be provided on demand).

## 2. MATERIAL AND MODELIZATION

### 2.1 Material

In order to emulate the LOR principle, we use a low friction Airpel<sup>®</sup> pneumatic cylinder coupled with a Festo MPYE<sup>®</sup>-5-M5-010 B servo-valve. In order to set up our control laws we use a position sensor and two pressure transducers (MEAS<sup>®</sup> U5136), one for each cylinder chamber. In this context, the pneumatic cylinder is the equivalent of the syringe used in the original operation and the plunger is equivalent to the piston of this cylinder. In order to emulate the LOR principle we needed to have a precise model of the system so that it is possible to render the feeling of this loss of resistance. A simplified diagram of the pneumatic cylinder is depicted in Fig.1. In this diagram,  $S$  is the piston surface which, in our case, is the same in both chambers, both  $q_m$  represent mass flows,  $V_N$  and  $V_P$  volumes,  $P_N$  and  $P_P$  pressures and  $T$  temperatures. The subscripts refer to the chamber of the cylinder. Finally  $F_{dist}$  represents the force applied on the cylinder by the user as if he pushed the plunger of a syringe.

### 2.2 System modeling

The model of the system is mainly based on the one proposed by Abry et al. (2013). This model is based on a classical thermodynamical modeling in which the author added an A-T transform based on Park transform usually used in electrical design. This transform is presented in eq.(1).

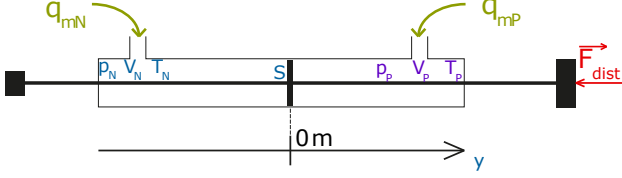


Fig. 1. Simplified diagram of the test bench pneumatic cylinder variables

$$\begin{bmatrix} q_{mA} \\ q_{mT} \end{bmatrix} = \Lambda(y) \cdot \begin{bmatrix} q_{mP} \\ q_{mN} \end{bmatrix} \quad (1)$$

where

$$\Lambda(y) = V_0 \cdot \begin{bmatrix} \frac{1}{V_P} & -\frac{1}{V_N} \\ \frac{1}{V_P} & \frac{1}{V_N} \end{bmatrix} \quad (2)$$

In eq.(1),  $q_{mA}$  represents the active flow (which provokes a pneumatic force due to a difference of pressurization of both chambers),  $q_{mT}$  represents the pressurization flow (which provides a different stiffness to the piston when pushed by the user),  $q_{mP}$  and  $q_{mN}$  are the input mass flows in both chambers.  $V_N$  and  $V_P$  are the volumes of each chambers,  $y$  is the position of the piston and  $V_0$  is the total volume of the cylinder.

This modeling provides an easy mean to render a position control and also a force control. This model, presented in eq.(3), allows for two different types of control. First, the control law offered by Abry et al. (2013) controls the position of the piston over time with two parameters: a closed-loop damping and a closed loop stiffness. For our simulation we needed to control the damping of the motion. A high damping can create a high resistance force and a low damping can render a low resistance force. However the damping provided by the control law was not sufficient to achieve this. Then the control law has been utilized with a tweak that allows us to emulate a variable damping using the closed loop stiffness parameter. The second type of control law aims at reproducing a pneumatic force equivalent to the resistance force felt by the user when pushing the plunger.

$$\begin{cases} \frac{dy}{dt} = v \\ \frac{dv}{dt} = \frac{-b \cdot v - F_{fr}(v) + F_{pneu}}{M} \\ \frac{dF_{pneu}}{dt} = -K_{pneu} \cdot v + B_1 \cdot q_{mA} \end{cases} \quad (3)$$

In eq.(3),  $q_{mA}$  represents the control input,  $v$  the velocity of this piston,  $b$  the physical damping of the cylinder,  $F_{fr}$  the friction force,  $F_{pneu}$  the pneumatic force,  $M$  the mass of the piston,  $K_{pneu}$  the pneumatic stiffness,  $B_1 = \frac{k \cdot r \cdot T \cdot S}{V_0}$  a constant,  $k$  the polytropic constant,  $r$  the piston radius,  $V_0$  the total volume. These variables are represented in Fig.1.  $K_{pneu}$  expression is provided in eq.(3bis)

$$K_{pneu} = \left( \frac{P_P}{V_P} + \frac{P_N}{V_N} \right) \cdot k \cdot S^2 \quad (3bis)$$

Here  $P_P$  and  $P_N$  represent the pressure in each chambers, as stated in Fig.1.

### 3. CONTROL LAWS

Based on the model presented in eq.(3), two control approaches have been created, one based on the work of Abry et al. (2013) and using a position control to emulate a variable damping and the other controlling the pneumatic force,  $F_{pneu}$  in order to reproduce the real resistance force.

#### 3.1 Emulation of a variable damping

Abry et al. (2013) introduced a position control law for pneumatic cylinders. This law is a backstepping law that has some parameters tied to the closed loop stiffness and damping of the final system. Thanks to these parameters, this control position law has inherent interest for our particular case. Indeed we can use the closed loop stiffness in order to generate the appropriate haptic response. This work presents the following control law:

$$q_{mA} = f_0 + f_1 \cdot z_1 + f_2 \cdot z_2 + f_3 \cdot z_3 \quad (4)$$

with:

$$\begin{aligned} f_0 &= \frac{M^2 \cdot j_d + M \cdot K_{pneu} \cdot v - v \cdot b^2 - b \cdot F_{sec} + F_{pneu} \cdot b}{M \cdot B_1} \\ f_1 &= -\frac{M \cdot (C_1^3 - 2 \cdot C_1 - C_2)}{B_1} \\ f_2 &= \frac{M^2 \cdot (C_1^2 + C_1 \cdot C_2 + C_2^2 - 1) - 1}{M \cdot B_1} \\ f_3 &= -\frac{C_1 + C_2 + C_3}{B_1} \end{aligned}$$

Here  $C_1$ ,  $C_2$ , and  $C_3$  are three positive parameters that have to be tuned depending on the expected performance of our law,  $j_d$  the desired jerk and  $z_1 = y - y_d$ ,  $z_2 = v - v_d + C_1 \cdot z_1$ ,  $z_3 = F_{pneu} - F_{pneu_d}$  the errors needed by the backstepping method. This control law sets a closed loop stiffness, as well as a closed loop damping, through the various parameters that has to be tuned. In Abry et al. (2013) it is shown that with this control law, the closed loop stiffness and damping can be respectively written:

$$K_{cl} = M \cdot (C_1 \cdot C_2 + 1) \quad (5)$$

and

$$B_{cl} = M \cdot (C_1 + C_2) \quad (6)$$

At first we tried to control only the damping by way of the value of  $B_{cl}$  but we could not get a proper control of the damping of the system during all the piston motion. But, when combining this equation with the fact that it is possible to get the stiffness of a system with:

$$K_{cl} = \frac{F_{dist}}{\Delta y} \quad (7)$$

(here  $F_{dist}$  is the disturbance force applied by the user while pushing the cylinder piston), it is possible to design a variable stiffness that renders a physical damping. Indeed with a physical damping we would get:

$$y = a \cdot t + b \quad (8)$$

as an expression of the piston position over time when the piston is pushed by the user with a constant force, and

where  $a$  can be assimilated to a physical damping,  $t$  is the time and  $b$  a constant that can be related to the initial conditions of the system. It is then possible to obtain this particular stiffness trajectory for our system:

$$K_{cl_d} = \frac{1}{\frac{1}{B_{cl_d}} \cdot (t - t_{in}) + \frac{1}{K_{cl_0}}} \quad (9)$$

Here  $K_{cl_d}$  is the desired closed loop stiffness,  $B_{cl_d}$  is the desired closed loop damping,  $t_{in}$  the time at which we record the pushing on the piston,  $K_{cl_0}$  the initial value for the closed loop stiffness, this is usually a high value around 3000 N/m.

To ensure stability of this law we need to make sure that  $K_{cl_d}$  has a minimum value strictly positive in time. We can for example choose this value to be around 200 N/m without hindering the results of this law. However, this law remains quite complex, due to the amount of parameters that need to be set in order for the law to work properly. This complexity turns out to be major setback when using it. In the end, simpler control laws have been developed to bypass this tuning issue.

### 3.2 A pneumatic force control

To avoid the tuning drawbacks of the previous law, pneumatic force control laws have been implemented to emulate the LOR principle. In this respect, two control laws have been developed using two different methods, a sliding mode control, based on a previous work from Shen and Goldfarb (2007), and a backstepping control. Both laws are solely based on this particular equation:

$$\frac{dF_{pneu}}{dt} = -K_{pneu} \cdot v + B_1 \cdot q_{mA} \quad (10)$$

These laws control the pneumatic force to render the resistance force needed to feel the loss of resistance. For these two laws we then define a desired pneumatic force,  $F_{pneu_d}$  as the objective of the control. Using eq.(10) we define a backstepping control law with this active flow:

$$q_{ma} = \frac{1}{B_1} \left( K_{pneu} \cdot v + \dot{F}_{pneu_d} \right) - C_{bsf} \cdot z_f \quad (11)$$

Here  $C_{bsf}$  is a positive parameter of our control law and  $z_f = F_{pneu} - F_{pneu_d}$  is the error for the backstepping control. Finally, based on Shen and Goldfarb (2007), we define a similar kind of control using a sliding mode approach:

$$q_{ma} = B_1^{-1} (\dot{F}_{pneu_d} + K_{pneu} \cdot v - \kappa \cdot \text{sgn}(s)) \quad (12)$$

Here  $s$  is the sliding surface defined as such:  $s = F_{pneu} - F_{pneu_d}$  and  $\kappa$  a parameter to choose. The final idea with these two laws is to choose the pneumatic force according to the resistance force we need to render the LOR haptic feedback.

## 4. PROTOCOL AND EXPERIMENTAL RESULTS

### 4.1 Protocol

Both control laws have been thoroughly tested in simulation prior to being implemented on our test bench. Various tests have been performed, such as step response, response

to a sine wave, disturbance rejection and finally simulation of the LOR principle. All results are quite encouraging for both step response, response to a sine wave and disturbance rejection with the pneumatic force control. It is not the case for the damping emulation for which it has been difficult to get good results for stiffness control.

We introduce the results of the LOR simulation, for the force control by sliding mode in Fig.3, the force control by backstepping in Fig.4 and the damping simulation control by backstepping in Fig.5. To simulate the LOR principle, the cylinder length is divided in two parts. The first part (from 0.035 m to  $-0.02$  m for the force control and from 0.035 m to 0 m for the damping emulation) represents the highly resistant part and the second part (from  $-0.02$  m to  $-0.04$  m for the force control and from 0 m to  $-0.04$  m for the damping emulation) is the less resistant part. At first the piston is fully pulled into the resistant part. When the user pushes on the piston, he feels a strong resistance force. Then, when the piston arrives at frontier position, the desired force or damping changes to create a lower resistance force. At this moment the user must realize that he is at the point of loss of resistance and stop pushing on the piston. If the moment of LOR triggering is clear to the user then the simulation is successful.

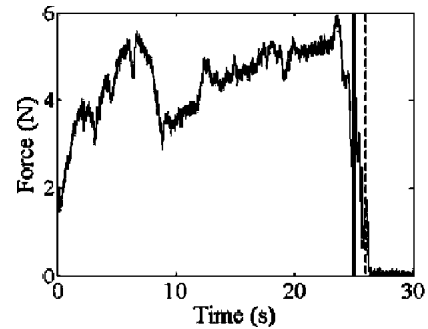


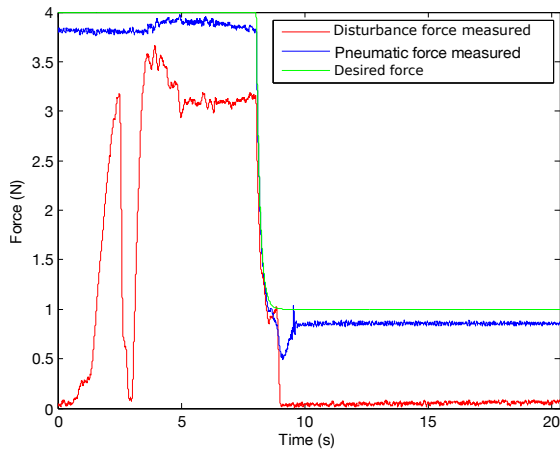
Fig. 2. Experimental measures of the resistance force applied on the plunger of an epidural syringe (Tran et al. (2009))

### 4.2 Discussion

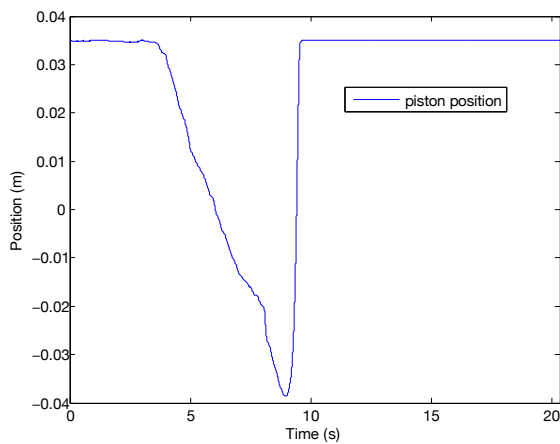
The results presented in Fig. 3 and Fig. 4 show a very good response both in terms of step response and disturbance rejection for the force control laws.

In these figures, we present the disturbance force applied by the user on the cylinder piston, the desired pneumatic force during the test, and the actual pneumatic force generated by the pneumatic cylinder. These results show that these laws are perfectly able to cope with a disturbance force without creating a high relative error. The different tests have shown the sliding mode chattering was an issue so the backstepping law provides a better quality haptic feedback.

The damping control law provides the results presented in Fig. 5. The stiffness control is not accurate with this type of control which hinders the accuracy of the damping control. Though, observing the pneumatic force generated in response to the disturbance force, it remains close to the experimental force measured in Tran et al. (2009) and depicted in Fig. 2. Moreover the haptic feedback also allows



(a)



(b)

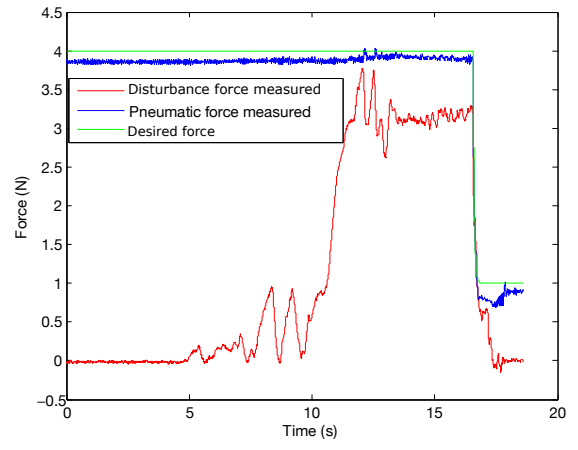
Fig. 3. (a) Disturbance force, pneumatic force recorded, and desired force for the Sliding mode control law (b) Position of the piston during this test

the user to detect the occurrence of the LOR principle. The difference between this law and the others is that the damping control law allows only a smooth transition between the high resistance and the low resistance parts. It still bears interest to render some of the hardest cases when the transition must be rendered unclear and the LOR triggering may be more subtle.

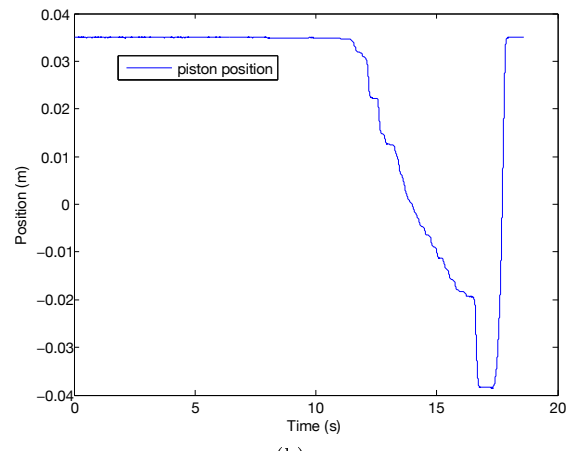
Finally, these control laws have been tested by an anaesthetist in order to validate the haptic feedback, to state whether the haptic feedback is close enough to the real haptic feedback of a syringe. His intervention also helped to tune some control parameters such as the norm of the resistance force,  $F_{pneu,d}$ , or the damping,  $B_{cl,d}$ , needed to emulate the feeling of the real syringe. The tests have brought very interesting results showing that this hardware simulation was close enough to the reality to be considered usable as a part of a complete simulator.

## 5. CONCLUSION

Both force control laws ended up giving very good experimental results and providing a high quality haptic feedback for the user. As far as the simulation of the LOR principle is concerned these laws provide a very good control of the haptic feedback. In the example depicted



(a)



(b)

Fig. 4. (a) Disturbance force, pneumatic force recorded, and desired force recorded for the Backstepping control law (b) Position of the piston during this test

in this paper, for the force control laws we used filtered step inputs as a way to prevent an overshoot in the pneumatic force response. This filtering allows to control the pneumatic force decrease speed and thus to control the haptic feedback efficiently. For example, it can be used to emulate different kinds of patients (aged, calcified, ...) and create a more realistic LOR simulation. To widen the range of application of these results, this force control law may also be used for any simulation of a syringe. In our case it should be used in the future to simulate the syringe of various articular puncture operations.

## REFERENCES

- Abry, F., Brun, X., Sesmat, S., and Bideaux, E. (2013). Non-linear position control of a pneumatic actuator with closed-loop stiffness and damping tuning. In *European Control Conference (ECC)*, 1089. Zürich, Switzerland.
- Dang, T., Annaswamy, T.M., and Srinivasan, M.A. (2001). Development and evaluation of an epidural injection simulator with force feedback for medical training. *Studies in Health Technology and Informatics*, 81, 97–102.
- Magill, J., Anderson, B., Anderson, G., Hess, P., and Pratt, S. (2004). Multi-axis Mechanical Simulator for Epidural Needle Insertion. In *Medical Simulation*, 267–276. Springer Berlin Heidelberg. DOI: 10.1007/978-3-540-25968-8\_30.

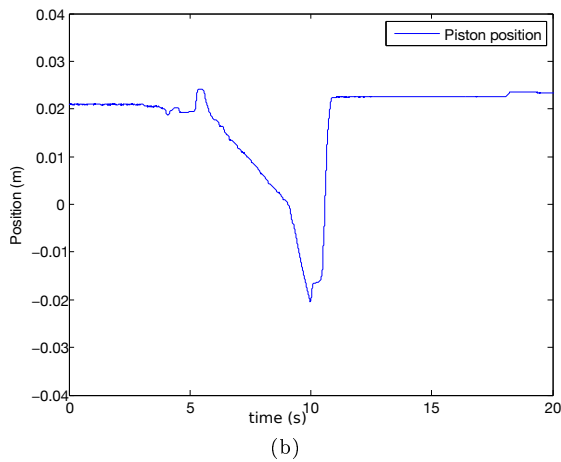
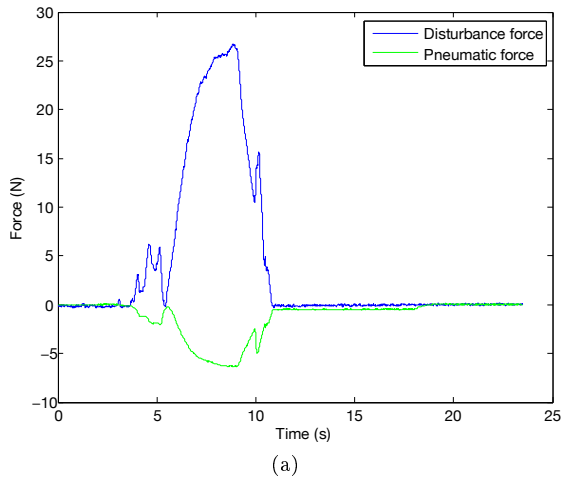


Fig. 5. (a) Disturbance and pneumatic force recorded for the Backstepping control law (b) Piston position during the test (the most resistant part is for a position between 0.04 m and 0 m and the least resistant part is between 0 m and  $-0.04$  m)

Shen, X. and Goldfarb, M. (2007). Simultaneous Force and Stiffness Control of a Pneumatic Actuator. *Journal of Dynamic Systems, Measurement, and Control*, 129(4), 425. doi:10.1115/1.2745850.

Tran, D., King-Wei Hor, Kamani, A., Lessoway, V., and Rohling, R. (2009). Instrumentation of the Loss-of-Resistance Technique for Epidural Needle Insertion. *IEEE Transactions on Biomedical Engineering*, 56(3), 820–827. doi:10.1109/TBME.2008.2011475.

Vaughan, N., Dubey, V.N., Wee, M.Y., and Isaacs, R. (2013). A review of epidural simulators: Where are we today? *Medical Engineering & Physics*, 35(9), 1235–1250. doi:10.1016/j.medengphy.2013.03.003. URL <http://linkinghub.elsevier.com/retrieve/pii/S135045331300057X>.

## Name Definition

HAS	Haute Autorité de la Santé
$F_{pneu}$	Pneumatic force (N)
$S$	Piston area (m)
$p_N, p_P$	Pressure in both cylinder chamber (bar)
$p_a$	Atmospheric pressure (bar)
$F_{fr}$	Friction force (N)
$y$	Piston position (m)
$v$	Piston velocity (m/s)
$V_N$ et $V_P$	Chamber volumes (m <sup>3</sup> )
$V_0$	Total volume (m <sup>3</sup> )
$T_P, T_N$	Temperature in each chamber (K)
$k$	Polytropic constant
$r$	Piston radius (m)
$q_{mP}, q_{mN}$	Air flows in each chamber (kg/s)
$q_{mA}$	Active massic air flows (kg/s)
$q_{mT}$	Pressurization massic air flow (kg/s)
$K_{pneu}$	Pneumatic stiffness (N/m)
$K_{cl}$	Closed loop stiffness (N/m)
$j_d, a_d, v_d, y_d, F_{pneu_d}$	Desired jerk (m/s <sup>3</sup> ), acceleration (m/s <sup>2</sup> ), velocity (m/s), position (m) and force (N)

## NOMENCLATURE